

# Pick-up Calibration in CESR Beam Position Monitors

Beau Meredith

*Department of Physics, Greenville College, Greenville, IL, 62246*

(Dated: August 9, 2003)

The beam position algorithm inside Cornell Electric Storage Ring (CESR) does not accurately resolve the position of the beam at large displacements from beam pipe center. To reduce this problem, a new beam position algorithm is being implemented. This paper discusses the implementation of this new algorithm, and also addition corrections made for misalignments of beam position monitor buttons.

## I. INTRODUCTION

Identifying the position of electron and positron bunches is a very important task of accelerator physics inside the Cornell Electric Storage Ring (CESR). Accurate positioning simplifies accelerator and luminosity tuning and enables simple testing of the magnetic elements inside the ring. The beam position monitors inside CESR consist of four button electrodes which measure a signal due to a charged bunch.

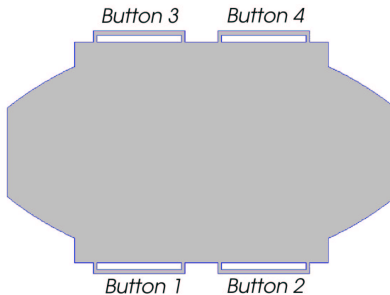


FIG. 1: 2D transverse cross section of Arc BPM used in CESR. The white rectangles represent the buttons and the grey area is the interior of the vacuum pipe.

The current method used to resolve the position assumes that combinations of the four signals  $s_i$  are proportional to the beam position and is termed the difference over sum method.

$$x = x_0 \frac{(s_2 + s_4) - (s_1 + s_3)}{\sum_i s_i} \quad (1)$$

$$y = y_0 \frac{(s_3 + s_4) - (s_1 + s_2)}{\sum_i s_i} \quad (2)$$

The difference over sum method [3] for converting bpm signals to position works well for beams in the center of the beam pipe, but the linear relationship breaks down at large displacements. The pretzel orbit in CESR causes large displacements and thus renders the difference over sum method ineffective. Here, I describe the implementation of a method that accurately resolves beam positions at large displacements from beam pipe center. For this, a new beam position algorithm based upon a 2D electrostatic model of the bpm's was installed. Furthermore, calibration coefficients were introduced that account for geometrical

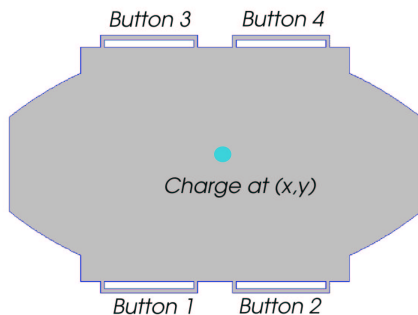
misalignment of bpm buttons. The two processes will first be briefly be described, followed by a description of their implementation and measurements that test their usefulness.

## II. 2D ELECTROSTATIC MODEL

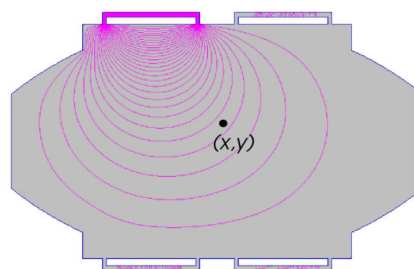
The 2D electrostatic model is designed to be a general solution for finding beam position that can be used for beams at an arbitrary transverse position in the beam pipe, whereas the linear difference over sum method is only accurate for small transverse displacements. The conditions necessary for generality and accuracy of the 2D method are ultra-relativistic speeds and sufficiently long beam bunches. When these conditions are met, the 3D problem of converting measured signals from the 3D bpm structure to transverse positions simplifies into a 2D electrostatic problem [1]. This simplification from a 3D electrodynamic problem to a 2D electrostatic one is the basis for the new bpm algorithm. One could solve this electrostatic problem directly for a large set of beam positions  $(x,y)$ , for each of which the induced signals on each of the buttons would be computed. One would then compare measured button signals to these calculations to obtain the horizontal and vertical beam position. However, this would be very inefficient and time consuming. Instead, a useful and efficient solution can be found that only utilizes one electrostatic calculation. For a more detailed presentation, see Helms [4].

Consider the two separate cases inside a beam position monitor:

1. A static charge at position  $(x,y)$  inside the BPM with all electrodes grounded
2. Placing a potential on button  $i$  with no charge inside the BPM and buttons  $j, j \neq i$  grounded



(a) Physical representation of case 1



(b) Physical representation of case 2

A relationship is given by Greene's Reciprocity theorem [4] that relates the induced surface charge on the button  $i$  in case 1 to the potential at  $(x,y)$  in case 2. Using this relationship for  $i=1\dots 4$ , we can find the position of the beam by

1. Solving for the potentials in case 2
2. Minimizing a  $\chi^2$  fit.

The a  $\chi^2$  fit involves the calculated potentials from case 2 and the measured signals off the buttons. The location that minimizes this fit is the calculated position of the beam. This is the method by which the measured signals are converted to position

The Poisson electrostatic field solver was used to solve for the potentials inside the bpms. To utilize Poisson, the different bpm geometries had to be plotted into a Poisson input file. Then, a voltage was placed on one of the buttons and Poisson calculated the potential throughout the interior a bpm. This was done for all different types of bpms used in CESR including Q0, Q1, Q2, Q48, Q49, and Arc. The mesh increments used in the input files for the bpms are shown in the table below.

TABLE I: Mesh sizes used for bpms

bpm	increment for x and y (cm)
Q0	0.015
Q1	0.015
Q2	0.03
Q48	0.015
Q49	0.015
Arc	0.01

### III. BUTTON MISALIGNMENT

The previous method is a general one, but it assumes that the buttons are perfectly aligned. That is, they are aligned exactly as specifications dictate. In reality, there are small differences between the actual and specified positions of the electrodes. For a given beam at a transverse position (x,y), these differences cause different signals to be measured at each button electrode, which in turn creates a small error in the calculated position of the beam. Corrections for these errors utilize a set of calibration coefficients that are unique to each BPM. A complete derivation of these correction factors can be found in [2][? ][? ].

If a beam passes through a bpm with misaligned button i, then the measured potential on button i will be  $\tilde{U}_i = b_i U_i$ , where  $U_i$  is the potential that would be induced on a perfectly aligned button, and  $b_i$  is the calibration coefficient associated with button i. The values of  $b_1, b_2, b_3, b_4$  can be used to improve beam position accuracy by including them into the aforementioned  $\chi^2$  minimization [Helms]. A major goal of this project was first to find these  $b_i$ s and second to include them into the algorithm for finding the beam position. To find the

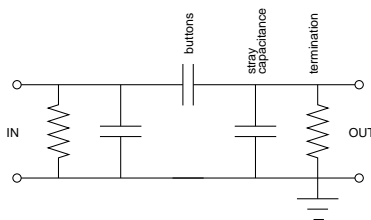


FIG. 2: Beam position monitor circuit diagram.

value of the each  $b_i$ , a spectrum analyzer was used to place a known RF signal on one button and measure the RF signal on another button. The buttons are separated by space and so the measurement is analogous to placing a potential on one plate of a capacitor and measuring the potential on the other plate. The measurement is related to the capacitive coupling of both buttons, and so it contains information about the misalignment of both buttons. Therefore, the measurement contains information about both  $b_i$  and  $b_j$ . Let the measured RF signal be  $\tilde{U}_{ij}$ , and the perfectly aligned button RF signal be  $U_{ij}$ . The relationship between the perfect button signal and measured signal is  $\tilde{U}_{ij} = b_i b_j U_{ij}$  [2]. To find  $b_1$ ,  $b_2$ ,  $b_3$ , and  $b_4$ , we must make six measurements,  $\tilde{U}_{12}$ ,  $\tilde{U}_{13}$ ,  $\tilde{U}_{14}$ ,  $\tilde{U}_{24}$ ,  $\tilde{U}_{23}$ ,  $\tilde{U}_{43}$ , that encompass all measurement combinations. Then we utilize the following two relationships of a bpm with perfectly aligned buttons:

1. The coupling between i and j is the same as between j and i, and hence  $\tilde{U}_{ij} = \tilde{U}_{ji}$  assuming the terminating resistances are all equal (which in theory they should be).
2. Physical symmetries dictate that  $U_{12} = U_{43}$ ,  $U_{13} = U_{24}$ ,  $U_{14} = U_{23}$  (Again assuming that the termination resistances are equal). This comes from the fact that the bpm's are symmetric about their horizontal and vertical axes.

We can then solve for each  $b_i$  in terms of  $b_1$ . The  $\chi^2$  minimization process uses ratios of  $b$ 's, so we are free to scale them arbitrarily. Setting  $b_1 = 1$  and solving for  $b_2$ ,  $b_3$ , and  $b_4$  yields the following:

$$b_1 = 1 \tag{3}$$

$$b_2 = \sqrt{\frac{\tilde{U}_{23}\tilde{U}_{24}}{\tilde{U}_{13}, \tilde{U}_{14}}} \tag{4}$$

$$b_3 = \sqrt{\frac{\tilde{U}_{23}\tilde{U}_{43}}{\tilde{U}_{13}, \tilde{U}_{14}}} \tag{5}$$

$$b_4 = \sqrt{\frac{\tilde{U}_{24}\tilde{U}_{43}}{\tilde{U}_{12}, \tilde{U}_{13}}} \tag{6}$$

The signal measured by the spectrum analyzer is the signal across the resistor, and hence  $\tilde{U}_{ij} = V_R$ . A simple RC series circuit has the relationship that  $V_R = \frac{V_{max}RC\omega}{\sqrt{1+(RC\omega)^2}}$ . When  $\omega \ll \frac{1}{RC}$ , then the relationship  $V_R = V_{max}RC\omega$  holds. Assuming a parallel plate capacitor model the button capacitance (a gross overestimation of the capacitance),  $frac{1}{RC}$  is near 100 GHz. Since the maximum  $\omega$  used is 100 MHz  $\ll \frac{1}{RC}$ , the spectrum analyzer measurements should produce an output voltage that is linearly proportional to  $\omega$ . Since all  $\tilde{U}_{ij}$  are linearly proportional to  $\omega$ , the quotients for the  $b_i$ 's in the eqns. (3) through (6) all cancel any dependence on  $\omega$ . Hence, only the slope of the RF signal vs.  $\omega$  curve needs to be known. Therefore, all measurements consist of measuring the slope of a  $\tilde{U}_{ij}$  vs.  $\omega$  curve.

#### IV. PROCEDURE

The calibration coefficients for each bpm in the CESR ring were measured using an HP3588 Spectrum Analyzer. The buttons not involved in a particular measurement were

grounded with of shorting caps. Each measurement was made by putting a known RF signal on one button and measuring the the RF signal on another button with a frequency sweep of 1 to 100 MHz. The circuit diagram for the bpm simplifies to a simple series RC circuit, and so we expected and observed a fairly linear signal response curve. The rationale for using the 1-100 MHz span was that outside these bounds the measurements stopped being linear. Possible causes include standing waves inside the coax cables, cable interference, and outside noise. Each measurement consisted of averaging 70 individual measurements using the exponential averaging feature available on the spectrum analyzer.

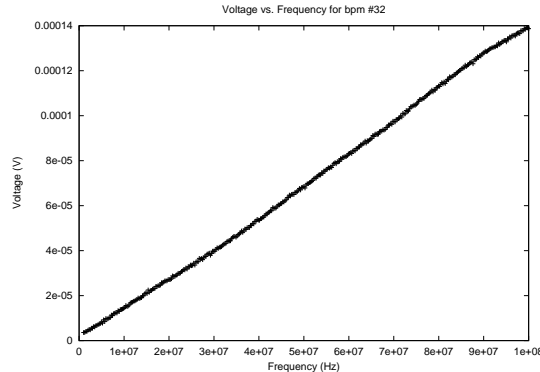


FIG. 3: Sample spectrum analyzer measurement.

## V. PROCEDURAL NOTES

Because of the symmetry argument made in the BPM Coefficients section, only six measurements were performed. However, this assumed that all terminating resistances were identical. In reality, they are not identical and can vary up to 1 ohm (most are still very close). This affects the theoretical argument in two ways:

1. The order in which the measurements are taken is important.
2. If only six measurements are taken, all the values of the termination resistors must be known.

The termination resistances were obtained off the resistance boxes of each button and used in the calculation of  $b_i$ s. However, they did not significantly improve the fitting, and so their usefulness is questionable.

## VI. RESULTS OF CALIBRATION

The values of the calibration coefficients usually ranged from 0.93 to 1.07. Finding the position of a beam utilizes a  $\chi^2$  minimization (see 2D Electrostatic Model). For most bpm's, the  $\chi^2$  goodness of fit was smaller when the coefficients were used as compared to when they were not used. Analytical calculations indicate that a smaller  $\chi^2$  goodness of fit leads to better accuracy of beam position. This leads to the conclusion that the coefficients have improved the beam positioning system. However, there were bpm's where the  $\chi^2$  goodness of

fit did not improve when the coefficients were used. Calibration measurements were repeated on two of the faulty bpms. The new calibration data did not improve the  $\chi^2$  fits, and so it can be reasonably concluded that something other than the calibration coefficients are at fault.

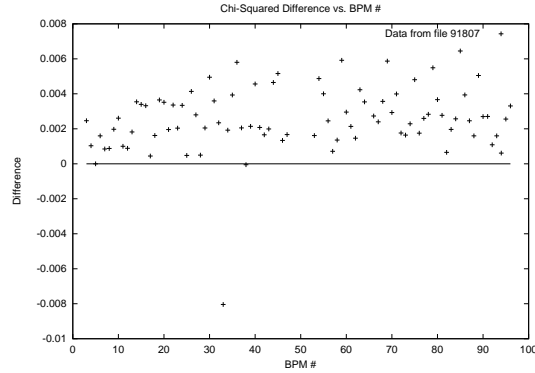
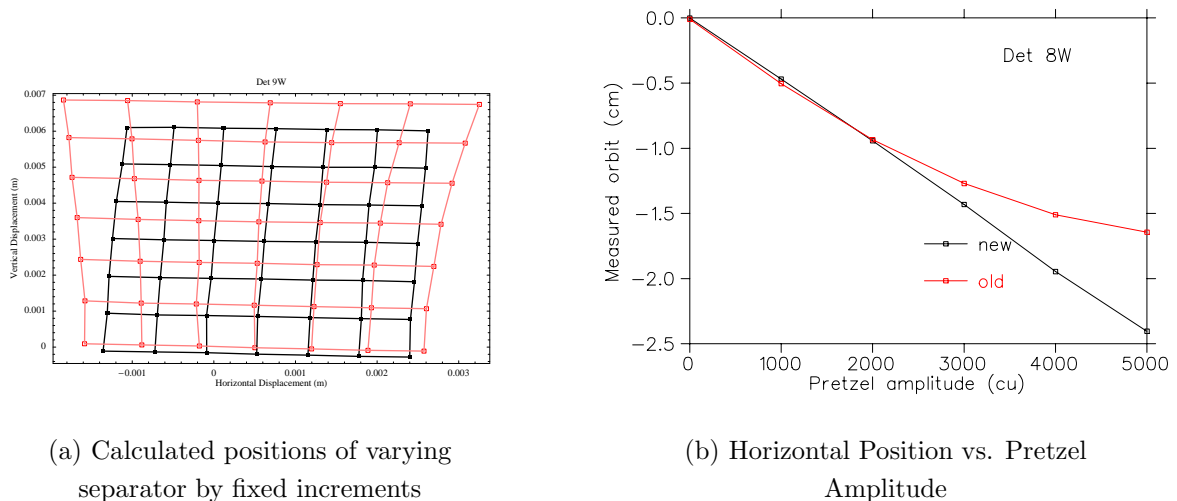


FIG. 4: Plot of difference in  $\chi^2$  fit when the coefficients are not used and when they are. The bpm number is on abscissa. The measurements were taken during one complete orbit in the ring.

## VII. TESTING

Two tests were performed with the new beam positioning algorithm.

1. Vary horizontal and vertical separator voltages by fixed increments and measure the position.
2. Vary pretzel amplitude and measure horizontal position.



(a) Calculated positions of varying separator by fixed increments

(b) Horizontal Position vs. Pretzel Amplitude

FIG. 5: Two tests done to test how well new algorithm works at large displacements from beam pipe center

The relationship between horizontal beam position and pretzel amplitude is linear. The plot of the pretzel amplitude shows that the old beam position algorithm became nonlinear at displacements of about 1 cm, whereas the new algorithm keeps its linear relationship out to the highest displacement shown. This linear relationship shows that the new algorithm is behaving as one would predict when varying the pretzel amplitude, and shows that the new algorithm is much more accurate at large displacements from beam pipe center.

Varying the horizontal and vertical separator voltages by fixed increments and calculating the resulting positions should yield a very uniform looking grid. This is because changes in separator voltages are linearly proportional to changes in position. The difference over sum calculated positions are shown in red, while the 2D electrostatic calculated positions are in black. At large displacements from beam pipe center, the edges of the difference over sum method begin to curve and show a nonlinear relationship between position and separator voltage. The 2D electrostatic method keeps a fairly linear relationship at the outer edges. This is further evidence that the new algorithm being implemented does in fact improve position resolution out to large displacements.

## VIII. CONCLUSIONS & RECOMMENDATIONS

Preliminary testing of the new beam position monitor algorithm used by CESR shows that it is more accurate than the old system in resolving the position of the beam at large displacements from the beam pipe center. In addition, the inclusion of the calibration coefficients seems to improve the positioning accuracy of the bpms. It is recommended to use the calibration coefficients on the bpms where the  $\chi^2$  of fit improves.

## IX. ACKNOWLEDGMENTS

I would like to thank graduate student Rich Helms and Professor Georg Hoffstaeter of Cornell University, who proposed this REU project and guided me through the experience. I would also like to thank Rich Galik for inviting me to this program. Special thanks goes to John Sikora, Bob Mellar, Jeremy Urban, Yulin Li, Jeff Smith, Mark Palmer, Charlie Strohl, and JK, for their help.

- 
- [1] J. H. Cuperus, Nuclear Instruments and Methods **220**, (1977) 145.
  - [2] J. Keil, Measurement, Correction, and Analysis of a Beam Position Monitor Electrode at ELSA, **67**, (2000).
  - [3] P. Bagley and G. Rouse, Calibration of a Beam Position Detector by Moving the Beam Pipe **1**, (1991).
  - [4] R. Helms, New Method of Beam Position Calculation, **1**, (2003).